Styrene–Butadiene Rubber/Cellulose II/Clay Nanocomposites Prepared by Cocoagulation—Mechanical Properties

Carmen Lane Giri Zine,[1] Alberto Justino da Conceição,[1] Leila L. Y. Visconte,[1] Edson Noriyuki Ito,[2] Regina C. R. Nunes[1]

[1]*Instituto de Macromoléculas Professora Eloisa Mano, Universidade Federal do Rio de Janeiro, PO Box 68525, Centro de Tecnologia, Bloco J, 21945-970 Rio de Janeiro, Brazil*
[2]*Universidade Federal do Rio Grande do Norte, Brazil*

Received 9 April 2010; accepted 21 August 2010
DOI 10.1002/app.33240
Published online 29 November 2010 in Wiley Online Library (wileyonlinelibrary.com).

ABSTRACT: In this work, nanocomposites of styrene butadiene rubber (SBR), cellulose II, and clay were prepared by cocoagulation of SBR latex, cellulose xanthate, and clay aqueous suspension mixtures. The incorporated amount of cellulose II was 15 phr, and the clay varied from 0 to 7 phr. The influence of cellulose II and clay was investigated by rheometric, mechanical, physicochemical, and morphological properties. From the analysis of transmission electron microscopy (TEM), dispersion in nanometric scale (below 100nm) of the cellulosic and mineral components throughout the elastomeric matrix was observed. XRD analysis suggested that fully exfoliated structure could be obtained by this method when low loading of silicate layers (up to 5 phr) is used. The results from mechanical tests showed that the nanocomposites presented better mechanical properties than SBR gum vulcanizate. Furthermore, 5 phr of clay is enough to achieve the best tensile properties. © 2010 Wiley Periodicals, Inc. J Appl Polym Sci 120: 1468–1474, 2011

Key words: nanocomposites; clay; mechanical properties; reinforcement; rubber

INTRODUCTION

Most application of elastomers would be impossible without the reinforcement by certain fillers, such as carbon blacks (CBs) or silica, both widely used as reinforcing fillers in the rubber industry. Reinforcement is usually associated with improvement in modulus, hardness, and tensile and tear strengths of vulcanized materials.[1,2] For a filler to behave as a good reinforcing agent, the three main factors, one must keep in mind, are particle size, structure, and surface characteristics. Rubber nanocomposites containing layered silicates (LS) as reinforcement have drawn the attention of researchers due to advantages that nanocomposites have over conventional composites.[3–19] The interest behind this development is placed on the nanoscale dispersion (the thickness of LS is ca. 1nm) and the very high-aspect ratio of the silicate platelets (length-to-thickness ratio up to 2000), which enable a high-reinforcing efficiency even at low-LS loading. To make the polar LS compatible with nonpolar polymers and thus to facilitate the LS exfoliation, the silicates are made organophilic.[4] This occurs by exploiting the cation exchange ability of the LS. Organophilic LS is, however, expensive, which forced researches to search for alternative methods. Pristine Clay is an inexpensive natural mineral.[19] In this sense, nonorganophilic (pristine) LS can be dispersed in water, which acts as swelling agent via hydration of the intergallery cations (usually Na^+ ions). Several rubbers are available in latex form, which is a rather stable aqueous dispersion of fine rubber particles (particle size below 5 μm). Mixing of latex with pristine LS, followed by coagulation, is therefore an interesting way to produce rubber nanocomposites.[7,10,12,14–19]

The possibility to obtain elastomeric nanostructured systems by introducing modified LS in different types of elastomers has been investigated as well.[3–6,8,11]

U.S. patent (065266,2005)[11] reports the preparation of nanocomposites comprised of water sellable clay particles in aqueous emulsions such as styrene butadiene rubber (SBR) or NR containing a novel amine to aid in the intercalation and partial exfoliation of the clay particles. The applications of such rubber nanocomposites are contemplated, for example, as aircraft tire tread, where a significant replacement of CB reinforcement is desired to reduce heat buildup for tire durability and to reduce tire weight for fuel economy.

Correspondence to: R. C. R. Nunes (rcnunes@ima.ufrj.br).
Contract grant sponsors: FAPERJ, CNPq, CAPES.

Organic fillers can also be used as rubber reinforcers.[20] Goettler et al.[21] recently studied the combination of discontinuous reinforcing elements at two different size scales in two polymer types—acrylonitrile-*co*-butadiene (NBR) elastomer and high-density polyethylene thermoplastic by melt-compounding approach for the clay incorporation. The two reinforcements were wood cellulose, with appropriate compatibilizing agents at the microscale that provided mechanical strengthening in tension, and organoclay at the nanoscale that enhanced stiffening and reduced failure propagation by tearing. Fibrous materials, such as cellulose short fibers, enhance the tensile properties of rubber compounds. In these cases, it is important to have homogeneous dispersions of the fibers throughout the rubber matrix to achieve improvement in the tensile properties of the vulcanized materials and also to avoid the formation of surface defects. Frequently, the poor fiber-matrix adhesion requires the use of a coating compound, compatible with both fiber and rubber. The utilization of regenerated cellulose (cellulose II), from cellulose xanthate as reinforcing material, not only makes the use of coatings unnecessary but also provides better tensile properties when compared with CB to vulcanized rubbers.[22–26] Nanocomposites of natural and synthetic rubbers with cellulose II have already been obtained by cocoagulation system as described earlier.[27–31]

In this work, SBR/cellulose II/clay nanocomposites were prepared by cocoagulating the mixture of rubber latex, cellulose xanthate, and clay aqueous suspension. The emulsion SBR is the most widely used rubber in the world, which is a result of its excellent balance of properties and cost.[32] Cellulose xanthate is a water-soluble intermediate in the production of viscose (rayon) and cellophane, materials from cellulose of wood pulp, or cotton.[33] The cost of xanthate solution with 9% of cellulose is around \$0.30–0.50 per kilogram. Cocoagulation of cellulose xanthate with various rubber latices is advantageous based on two aspects of technological interest.[29] First, the coprecipitation, even at low levels of xanthate, produces rubber powder with relatively uniform particle size, which can be easily processed using the technology for thermoplastics. Second, the cellulose acting as a reinforcing agent would lead to materials with properties of vulcanized rubber for industrial applications. The water-based cocoagulation method is also interesting from the economic point of view. Compared to the common method of mixing the filler into solid rubber by mechanical shear force, the compounding of rubber latex with clay and cellulose xanthate and then cocoagulation of the mixture saves energy, thus reducing the production cost.

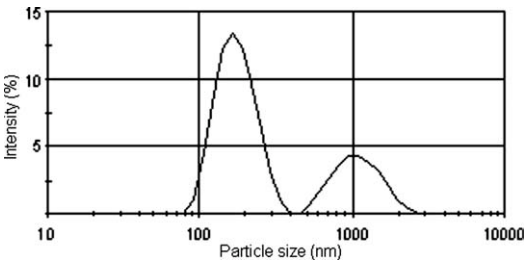

Figure 1 Particle size distribution of SBR latex.

EXPERIMENTAL

Materials

The SBR latex (S-62) with 23% bound styrene and 68% solid content was supplied by LANXESS Elastômeros do Brasil S.A., Duque de Caxias-RJ, Brazil. The latex particle size distribution, obtained by dynamic light scattering in a Zetasizer Nano-ZS (Malvern Instrument, Worcestershire, UK), is shown in Figure 1. The cellulose xanthate was supplied by Vicunha Têxtil S.A., Americana-SP, Brazil, with the following characteristics: 9.6% cellulose, 6.0% NaOH, and 84.4% H_2O. The clay (pristine Na-bentonite) from Wyoming, EUA, with a cationic exchange capability of 80 meq/100 g and BET surface area 28.5 m^2/g, was supplied by Bentonit União Nordeste S. A. (BUN), Campina Grande-PB, Brazil. The rubber-compounding ingredients used in this study were of commercial grade, namely, zinc oxide, stearic acid, sulfur, diphenyl guanidine, dibenzothizole disulfide, tetramethyl thiuram disulfide, and irganox 1010 (tetrakis [methylene-3-(3, 5-di-*tert*-butyl-4-hydroxyphenyl-propionate)]).

Preparation of nanocomposites

Clay was dispersed in deionized water under vigorous stirring (1% dispersion in water) during 2 h. Then, the clay aqueous suspension was added to the rubber latex and mixed for 20 min. After that, this mixture was poured onto the cellulose xanthate solution and stirred for a few minutes. Finally, the cocoagulation was carried out by adding, under stirring, SBR latex/cellulose xanthate/clay aqueous suspension mixture to an equimolar solution of sulfuric acid, and zinc sulfate. After coagulation, the fine SBR/cellulose II/clay particles were washed with deionized water to promote the removal of the residual acidity. The product was separated from the aqueous suspension by filtration and dried in an air-circulating oven at 50°C for 24 h. To prepare vulcanized nanocomposites, the mentioned nanocompounds as well as the gum SBR and the clay-free SBR/cellulose II were mixed with the appropriate ingredients, according to Table I, in a Berstorff two-roll mill at 50°C. The compounds were vulcanized in

TABLE I
Formulation for the Preparation of Nanocomposites

Material (phr)	Specific[a] gravity (g/mL)	SBR/cellulose II/clay				
		100/0/0	100/15/0	100/15/3	100/15/5	100/15/7
SBR	0.93	100	100	100	100	100
Cellulose II	1.62	0	15	15	15	15
Clay	2.43	0	0	3	5	7
Zinc oxide	5.40	5	5	5	5	5
Stearic acid	0.84	2	2	2	2	2
Sulfur	2.07	2	2	2	2	2
Dibenzothiazole disulfide	1.50	0.5	0.5	0.5	0.5	0.5
Diphenyl guanidine	1.19	0.5	0.5	0.5	0.5	0.5
Tetramethyl thiuram disulfide	1.40	0.2	0.2	0.2	0.2	0.2
Irganox 1010[b]	1.15	1	1	1	1	1

[a] Specific gravities were taken from refs. 34 and 35. The specific gravity of the clay was measured in an AccuPyc 1330 helium (He) Pycnometer (Micrometics Instruments Corporation).
[b] Tetrakis [methylene-3-(3,5-di-*tert*-butyl-4-hydroxyphenyl-propionate)].

a standard mold at 150°C in an electrically heated hydraulic press for the optimum cure time determined on an oscillating disk rheometer. From the resulting vulcanized sheets, samples for the mechanical tests were cut.

Characterization of nanocomposites

For transmission electron microscopy (TEM) measurements, 25-nm sections were microtomed at −80°C with cutting rate of 0.1 mm/s using RMC ultramicrotome model MT 7000 with a Diatome diamond knife model CryoHisto 45°. Measurements were carried out on a Philips CM120 TEM using an acceleration voltage of 120 kV.

Wide-angle X-ray diffraction measurements were carried out on a Miniflex Rigaku diffractometer with a scan rate of 0.5°/min, Cu Kα ($\lambda = 1.5418$ Å) radiation at 30 kV and 15 mA and 2θ scan range from 2 to 40°.

The maximum and minimum torques were determined according to ASTM D 2084 on an Oscillating Disk Rheometer, model TI 100 from Tecnologia Industrial, operating at 150°C and 1° arc. The tension and tear tests were performed in a model DL3000 EMIC Universal Testing Machine at a crosshead speed of 200 and 500 mm/min, respectively, at room temperature, using specimens punched out from the molded vulcanized sheets. Tensile testing followed standard DIN 53504 using S2 specimens. The tear strength was measured on unnotched 90° angle test specimen, according to ASTM D 624. The median value, measured over five specimens, was taken as the test result for each compound tested. The hardness was determined using a Shore A hardness, according to standard ASTM-D 2240 procedure.

The crosslink density was determined from equilibrium swelling in toluene at room temperature using the Flory–Rehner equation.[36] Small specimens ($2.0 \times 2.0 \times 0.2$ cm) dried to constant weight were allowed to swell in the dark in sealed bottles until no further swelling occurred. The swollen samples were weighed after removal of excess swelling agent and dried to constant weight. The volume of imbibed toluene was calculated from the difference between the weights of swollen and deswollen samples divided by the solvent density. Then, the dry samples were weighed in methanol, and their volumes calculated. From this volume, the volume of fillers (calculated from the recipe and original sample weight) was subtracted to give the volume of rubber. The latter was used to calculate the volume fraction of rubber in the swollen polymer[37] (V_r). The interaction parameter value for SBR–toluene systems[35] was taken as 0.31, and the molar volume of the solvent[38] was equal to106.29 mL/mol.

RESULTS AND DISCUSSION

Structure of SBR/cellulose II/clay nanocomposites

Figure 2 shows TEM micrographs of the SBR/cellulose II/clay nanocomposite containing 5 phr of clay at two magnifications. In Figure 2(a), it is possible to note the excellent dispersion of cellulose II in the rubber matrix. In Figure 2(b), the dark lines are the intersections of the silicate layers. Both, cellulose and clay are dispersed at nanolevel in the rubber matrix. Therefore, the cocoagulation can be considered as effective and applicable to rubbers in latex form.

XRD is a conventional method to determine the interlayer spacing of clay layers and was used to investigate the original clay and the polymer/LS nanocomposites. The XRD patterns of pristine clay and the nanocomposites with different clay contents are presented in Figure 3.

Results in Figure 3 suggest that in the nanocomposites prepared with 3 and 5 phr of clay, silicate

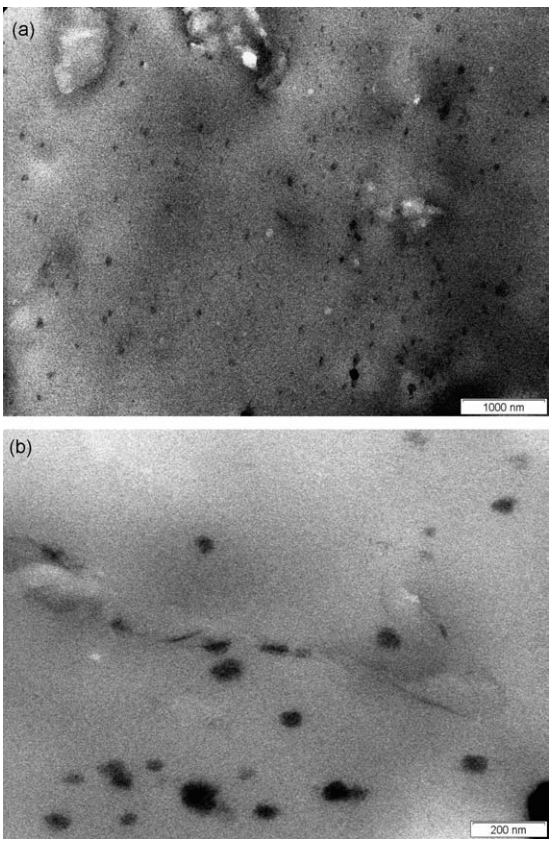

Figure 2 TEM micrographs of SBR/cellulose II/clay nanocomposite with 5 phr of clay at two magnifications.

layers are completely exfoliated. The bentonite clay showed a characteristic diffraction peak at $2\theta \approx 6.5^\circ$, which corresponded to an intergallery distance of 1.35 nm. The peak of the nanocomposite with 7 phr of clay appeared at $2\theta \approx 6.25^\circ$, which corresponded

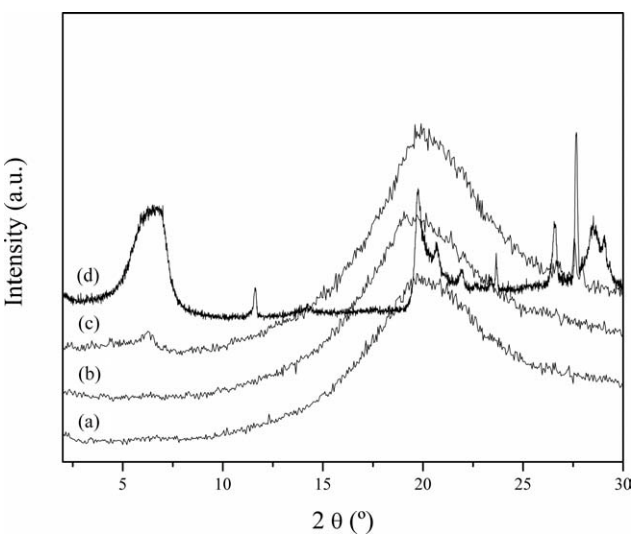

Figure 3 XRD patterns of SBR/cellulose II/clay cured nanocomposites with different clay contents and pristine clay: (a) 3 phr clay; (b) 5 phr clay; (c) 7 phr clay; (d) pristine clay.

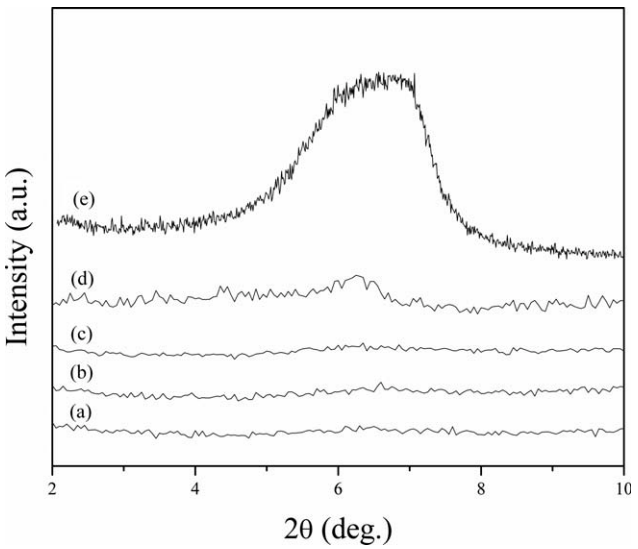

Figure 4 XRD patterns of four stages of the preparation process and pure clay: (a) stage 1, 1% clay aqueous suspension; (b) stage 2, mixture of SBR latex with clay aqueous suspension; (c) stage 3, mixture of SBR latex with clay aqueous suspension and cellulose xanthate solution; (d) stage 4, product after cocoagulation; (e) pristine clay.

to an intergallery distance of 1.41 nm. This value is larger than the initial one of bentonite clay (1.35 nm), which seems to indicate that rubber molecules are intercalated in between the clay interlayers. However, the increment in basal spacing is not large enough to allow the conclusion that the intercalation of rubber macromolecules into the interlayer occurred. This increment in basal space by cocoagulation can be thought of as being originated from the cations of the flocculant in the intergallery and not from intercalated rubber molecules into clay galleries. Based on the results from Wu et al.[10], the cation exchange reaction would occur during the cocoagulation process.

According to the XRD curves observed for nanocomposites containing 3 and 5 phr of clay, it was concluded that a partially exfoliated structure might be existing in the nanocomposite with 7 phr of clay. If intercalation of rubber chains into the interlayer of clay actually occurs, XRD peak for the intercalated nanocomposites will be shifted to a smaller angle, and if the clay layers are completely exfoliated, no diffraction peaks will be observed as either the sheets will be disordered or the layers will be largely spaced, beyond the XRD resolution. In this preparation method, in the latex, the nanodispersed structure is formed even when no polymer chain is present to intercalate in between the galleries. This subject has been completely investigated by Wu et al.[10] and is quite different from the well-known intercalated and exfoliated structures. Thus, to confirm the nanodispersed structure and better understand the mechanism of the nonintercalated

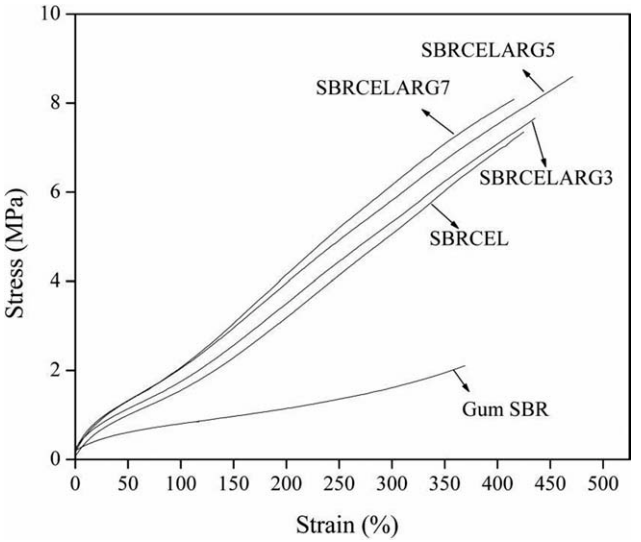

Figure 5 Stress–strain curves of SBR (gum) and the nanocomposites with cellulose II and different clay contents.

structure formation, we traced the preparation process of the SBR/cellulose II with 7 phr clay.

Figure 4 shows the XRD patterns at four stages of the preparation process. The first stage [Fig. 4(a)] is 1% clay aqueous suspension, and no XRD peak appears, which indicates the complete exfoliation of clay in water. The second stage [Fig. 4(b)], when the SBR latex was mixed with the clay aqueous suspension, again, no XRD peak appears, thus suggesting that the mixture is stable, and the rubber latex particles do not cause the aggregation of silicate layers. The third stage [Fig. 4(c)], after mixing with cellulose xanthate, still, no XRD peak appears. In the fourth stage [Fig. 4(d)], after cocoagulation, the XRD peak corresponding to the regular stacking of silicate layers appears, which indicate that the individual silicate layers dispersed in the mixture reaggregate during the process of cocoagulation.

Properties of SBR/cellulose II/clay nanocomposites

Stress–strain curves for SBR/cellulose II/clay nanocomposites with different clay contents are given in Figure 5. From these curves and the results in Table II, it is clear that the tensile strength property was improved upon the addition of cellulose II to the rubber matrix and reached about 300% that of the gum SBR. Additional improvement, although not so large, can also be seen on introduction of clay. With an increase in the clay amount from 3 to 5 phr, the tensile strength of the nanocomposite increases slightly and reaches about 396% compared to gum SBR. Further clay addition lead to a decrease in the property, but the value was still higher than that for the unfilled rubber. From these results, it can be said that 5 phr of clay is enough to achieve the best tensile properties concerning the SBR/cellulose II/clay nanocomposites.

The values of all mechanical properties evaluated in this work are shown in Table II. The energy at break was higher in comparison with the gum SBR as the combination of cellulose II and clay improved the toughness of the SBR matrix. The incorporation of cellulose II in the rubber caused a significant increase in the hardness of the nanocomposite, as expected, which is indicative of higher stiffness. The hardness also increased with the addition of clay, but the increase was not significant due the low-clay loading. The tear strength of the nanocomposites was excellent in comparison with gum vulcanizate and still increased with the amount of clay. Similar result was obtained by Lapa et al.[31] related to cellulose II. The authors studied the fracture behavior of nitrile rubber-cellulose II nanocomposites also prepared by cocoagulation. The fracture surfaces feature of tear test specimens suggested that the fracture propagation process occurs with a high-energy dissipation corroborating the good tear strength result. Cellulose II was dispersed at nanolevel without fiber alignment (Figure 2) differently from the short fibers composites obtained by another processing methods[39–41] where the fibers tended to align under the combined action of shear and elongational deformation. This kind of dispersed structure of cellulose II on rubber matrix by cocoagulation provided less anisotropy thus avoiding premature failure under transverse stresses. In addition, the sheetlike filler with large aspect ratio, a micrometer planar size, and nanometer thickness strongly limits the

TABLE II
Mechanical Properties of SBR and the Nanocomposites with Cellulose II and Different Clay Contents

Properties	SBR/cellulose II/clay				
	100/0/0	100/15/0	100/15/3	100/15/5	100/15/7
300% modulus	1.5 ± 0.16	4.9 ± 0.22	5.0 ± 0.26	5.8 ± 0.09	5.6 ± 0.31
Tensile strength (MPa)	2.17 ± 0.16	7.35 ± 0.54	7.66 ± 0.16	8.59 ± 0.08	8.09 ± 0.31
Elongation at break (%)	368 ± 45	422 ± 18	447 ± 14	468 ± 9	450 ± 27
Tear strength (kN/m)	12.30 ± 0.99	27.03 ± 2.89	32.94 ± 2.31	34.25 ± 2.24	38.58 ± 1.67
Hardness (shore A)	38 ± 0.6	51 ± 0.6	52 ± 0.8	57 ± 1.0	56 ± 1.0
Energy at break (N mm)	857 ± 144	2803 ± 279	3197 ± 90	4213 ± 221	3780 ± 294

TABLE III
Crosslink Density and Difference Between Maximum and Minimum Torques of SBR and the Nanocomposites with Cellulose II and Different Clay Contents

Sample	Crosslink density (mol/cm^3) $\times 10^{-3}$	$\Delta M = M_H - M_L$ (dN m)
SBR GUM	2.90 ± 0.05	21.69
SBR/CEL	3.73 ± 0.02	30.62
SBR/CEL/CLAY3	3.70 ± 0.03	31.07
SBR/CEL/CLAY5	4.01 ± 0.05	34.57
SBR/CEL/CLAY7	3.56 ± 0.05	31.52

deformation of macromolecules due to a highly efficient stress transfer.[7] Also, the clay layers can serve to reduce crack or tear propagation between the fibers.[21] Wang et al.[18] studied the influence of clay on rubber–clay nanocomposites mechanical properties and observed that tensile strength, hardness, and tear strength increased with increasing the clay content. The mechanical properties of the nanocomposites produced by the latex compounding method were better than those produced by the solution method. SBR-clay nanocomposites showed better mechanical properties than pure SBR and the other composites. The tear strength of SBR-clay nanocomposites was far higher than that of silica-reinforced SBR, which was attributed the especial layer structure of nanoclay[7]. Taking into account all evidence sources, it can be said that both clay and cellulose II, independently, dispersed at nanoscale in the rubber matrix improving the tear strength. The interesting gain in this property by combination of cellulose II and clay could be related to the new structure obtained by cocoagulation. However, further studies are necessary to verify the fracture behavior, especially the tear morphology, of SBR/cellulose II/clay nanocomposites.

The swelling measurements for the vulcanized rubbers in contact with organic solvents are used to determine the crosslinking density, which can be related to changes in physical properties. The effective additional crosslinks responsible for the reduced swelling in the filled vulcanizates presumably arise from a combination of several mechanisms. Possibilities that have been advanced include adhesion of the matrix through physical adsorption on the filler surface, chemical bonding of elastomer to the filler surface and formation of excessive polymer crosslinks at or near the surface of the filler by nonspecified catalytic effects.[42] A convenient and simple technique to study effects on cure rate and crosslinking is by using Oscillating Disk Rheometer data.[43] Crosslink density and the difference between maximum and minimum torques are shown in Table III. The crosslinking density of the gum SBR is increased by the addition of cellulose II. The Flory–Rehner method was used with correction for cellulose and clay presence, and so the solvent swelling results do correspond to crosslink density. With an increase in the clay amount to 5 phr, the crosslinking density increases. Further clay addition lead to a decrease in the property. These results agree with the difference between maximum and minimum torques, which is reflected in an increase in the strength of the elastomer. In fact, the combined cellulose II and clay behave as an effective reinforcing agent for SBR rubber.

From the above results, it can be assumed that the improvement in mechanical properties should be ascribed to an excellent dispersion of cellulose II and clay in the rubber matrix by the cocoagulation method.

CONCLUSIONS

The novel nanocomposites with light color obtained by combination of a mineral filler and cellulose II showed good reinforcement results in SBR vulcanizates. This could be attributed to the dispersion of cellulose II and clay at nanolevel in the rubber matrix by direct cocoagulating the rubber latex, cellulose xanthate, and clay aqueous suspension. In this work, 5 phr of clay was found to be enough to achieve the best tensile properties as far as the SBR/cellulose II/clay nanocomposites are concerned. The preparation process is simple, effective, and widely applicable to rubbers in the latex form.

The authors thank LANXESS Elastômeros do Brasil S.A. for supplying SBR latex, Vicunha Têxtil S.A. for supplying cellulose xanthate and Bentonit União Nordeste S. A. for supplying clay.

References

1. Wu, Y. P.; Jia, Q. X.; Yu, D. S.; Zhang, L. Q. Polym Test 2004, 23, 903.
2. Donnet, J. B. Compos Sci Technol 2003, 63, 1085.
3. Kim, W. S.; Yi, J.; Lee, D. H.; Kim, I. J.; Son, W. J.; Bae, J. W.; Kim, W. J Appl Polym Sci 2010, 116, 3373.
4. Chakraborty, S.; Kar, S. R.; Dasgupta, S.; Mukhopadhyay, R.; Bandyopadhyay, S.; Joshi, M.; Ameta, S. C. J Appl Polym Sci 2010, 116, 1660.
5. Choudhury, A.; Bhowmick, A. K.; Ong, C. J Appl Polym Sci 2010, 116, 1428.
6. Chakraborty, S.; Sengupta, R.; Dasgupta, S.; Mukhopadhyay, R.; Bandyopadhyay, S.; Joshi, M.; Ameta, S. C. J Appl Polym Sci 2009, 113, 1316.
7. Wu, Y.; Huang, H.; Zhao, W.; Zhang, H.; Wang, Y.; Zhang, L. J Appl Polym Sci 2008, 107, 3318.
8. Maiti, M.; Bhattacharya, M.; Bhowmick, A. K. Rubber Chem Technol 2008, 81, 384.
9. Sengupta, R.; Chakraborty, S.; Bandyopadhyay, S.; Dasgupta, S.; Mukhopadhyay, R.; Auddy, K.; Deuri, A. S. Polym Eng Sci 2007, 47, 1956.
10. Wu, Y. P.; Wang, Y. Q.; Zhang, H. F.; Wang, Y. Z.; Yu, D. S.; Zhang, L. Q.; Yang, J. Compos Sci Technol 2005, 65, 1195.

11. Goodyear Tire & Rubber Co. U.S. Pat. 065266 A1 (2005).
12. Wang, Y.; Zhang, H. F.; Wu, Y.; Yang, J.; Zhang, L. Q. Eur Polym J 2005, 41, 2776.
13. Karger-Kocsis, J. Polym Eng Sci 2004, 44, 1083.
14. Wu, Y. P.; Jia, Q. X.; Yu, D. S.; Zhang, L. Q. J Appl Polym Sci 2003, 89, 3855.
15. Varghese, S.; Karger-Kocsis, J. Polymer 2003, 44, 4921.
16. Utracki, L. A.; Kamal, M. R. Arab J Sci Eng 2002, 27, 43.
17. Wu, Y. P.; Zhang, L. Q.; Wang, Y. Q.; Liang, Y.; Yu, D. S. J Appl Polym Sci 2001, 82, 2842.
18. Wang, Y.; Zhang, L.; Tang, C.; Yu, D. J Appl Polym Sci 2000, 78, 1879.
19. Zhang, L.; Wang, Y.; Wang, Y.; Yuan, S.; Yu, D. J Appl Polym Sci 2000, 78, 1873.
20. Goettler, L. A.; Shen, K. S. Rubber Chem Technol 1983, 56, 619.
21. Goettler, L. A.; Benes, M.; Marko, M. H. Compos Interf 2009, 16, 599.
22. Mano, E. B.; Nunes, R. C. R. Eur Polym J 1983, 19, 919.
23. Nunes, R. C. R.; Mano, E. B. Polym Compos 1995, 16, 421.
24. Costa, V. G.; Nunes, R. C. R. Eur Polym J 1994, 30, 1025.
25. Vieira, A.; Nunes, R. C. R.; Visconti, L. L. Y. Polym Bull 1996, 36, 759.
26. Vieira, A.; Nunes, R. C. R.; Costa, D. M. R. Polym Bull 1997, 39, 117.
27. Martins, A. F.; Visconte, L. L. Y.; Schuster, R. H.; Boller, F.; Nunes, R. C. R. Kautsch Gummi Kunstst 2004, 57, 446.
28. Martins, A. F. PhD Thesis, Instituto de Macromoleculas Professora Eloisa Mano, Universidade Federal do Rio de Janeiro, Brazil.
29. Peres, E. C. C.; Nunes, R. C. R.; Visconte, L. L. Y. PI 0105116–4 (2001).
30. Brandt, K.; Schuster, R. H.; Nunes, R. C. R. Kautsch Gummi Kunstst 2006, 59, 511.
31. Lapa, V. L. C.; Suarez, J. C. M.; Visconte, L. L. Y.; Nunes, R. C. R. J Mater Sci 2007, 42, 9934.
32. Haynes, A. C. In Handbook of Elastomers; Bhowmick, A. K., Stephens, H. L., Eds.; Marcel Dekker: New York, 1988; Chapter 26, pp 761–774.
33. Wilkes, A. G. In Regenerated Cellulose Fibres; Woodings, C., Ed.; CRC Press: New York, 2000; Chapter 3, pp 37–57.
34. Alphen, J. V. In Rubber Chemicals; Turnhout, C. M. V., Ed.; Reidel: Boston, 1973.
35. Brandrup, J.; Immergut, E. H.; Grulke, E. A. Polymer Handbook, 4th ed; Wiley: New York, 1999.
36. Flory, P. J. Principles of Polymer Chemistry; Cornell University: New York, 1953.
37. Kraus, G. Rubber World 1956, 135, 67.
38. Lide DR, Ed. CRC Handbook of Chemistry and Physics. CRC Press: New York, 1997; p 3–55.
39. Goettler, L. A.; Sezna, J. A.; DiMauro, P. J Rubber World 1982, 187, 33.
40. Coran, A. Y.; Boustany, K.; Hamed, G. J Appl Polym Sci 1971, 15, 2471.
41. Kumar, R. P.; Thomas, S. Polym Int 1995, 38, 173.
42. Berriot, J.; Martin, F.; Montes, H.; Monnerie, L.; Sotta, P. Polymer 2003, 44, 1437.
43. Coran, A. Y. Science and Technology of Rubber; Academic Press: London, 1994.